Original Research

Elevated RUNX1 is a prognostic biomarker for human head and neck squamous cell carcinoma

Xiaodong Feng[1,*], Zhiwei Zheng[2,*], Yi Wang[1], Guanghui Song[1], Lu Wang[3], Zhijun Zhang[4], Jinxia Zhao[1], Qing Wang[1] and Limin Lun[1]

[1]Department of Clinical Laboratory, The Affiliated Hospital of Qingdao University, Qingdao University, Qingdao 266000, China; [2]Department of Oral and Maxillofacial-Head and Neck Oncology, Shanghai Ninth People's Hospital, Shanghai Jiao Tong University School of Medicine, Shanghai 200011, China; [3]Department of Education and Training, The Affiliated Hospital of Qingdao University, Qingdao University, Qingdao 266000, China; [4]Department of Clinical Laboratory, Taian City Central Hospital, Taian 271000, China
Corresponding author: Limin Lun. Email: lunlmqd@163.com
*These authors contributed equally to this paper

Impact statement

Head and neck squamous cell carcinoma (HNSCC) has been increased rapidly in China. New biomarkers are thus much needed to better predict tumor recurrence and prognosis. Previous studies have suggested that RUNX1 functions in mammalian hematopoietic development, thus regulating translocation-mediated leukemia. In this study, we demonstrate that RUNX1 could be used as a sensitive biomarker for tumor recurrence and prognosis in HNSCC patients.

Abstract

Runt-related transcription factors regulate many developmental processes such as proliferation and differentiation. In this study, the function of the runt-related transcription factor 1 (RUNX1) was investigated in head and neck squamous cell carcinoma (HNSCC). Our results show that RUNX1 expression was elevated in HNSCC patients, which was greatly correlated with the N stage, tumor size, and American Joint Committee on Cancer stage. Cox proportional hazard models showed that RUNX1 could be used as a prognostic indicator for the overall survival of HNSCC patients (hazard ratio, 5.572; 95% confidence interval, 1.860–9.963; $P < 0.001$). Moreover, suppression of RUNX1 inhibited HNSCC cell proliferation, migration, and invasion. Using the HNSCC xenograft nude mouse model, we found that the shRUNX1-transfected tumor (sh-RUNX1) was significantly smaller both in size and weight than the control vector-transfected tumor (sh-Control). In conclusion, our results show that the elevated RUNX1 expression was correlated with tumor growth and metastasis in HNSCC, indicating that RUNX1 could be used as a biomarker for tumor recurrence and prognosis.

Keywords: Head and neck squamous cell carcinoma, RUNX1, prognosis, migration

***Experimental Biology and Medicine* 2021; 246: 538–546. DOI: 10.1177/1535370220969663**

Introduction

Head and neck squamous cell carcinoma (HNSCC) is a collective of cancer found in many locations, including larynx, pharynx, and oral cavity, which accounts for approximately 3% of annual cancer incidence worldwide.[1] Although many new therapeutic improvements have been proposed for treating HNSCC, the long-term survival rate remains low due to the recurrence of tumor and metastasis.[2] To develop new treatments toward HNSCC, many efforts have been devoted to the molecular mechanisms of HNSCC progression.

Runt-related transcription factors (RUNXs)[3,4] regulate many developmental processes, such as cell proliferation and apoptosis.[5] Among the RUNXs, RUNX1 has been extensively investigated, which has been found to function in the generation of hematopoietic stem cells.[6,7] RUNX1 has recently been shown to regulate transcription by binding to core binding factor β (CBFβ).[8] This RUNX1/CBFβ complex activates or represses the transcription of many important regulatory factors of cell survival, proliferation, or differentiation.[9] More importantly, RUNX1 plays important roles in the regulation of mammalian hematopoietic development and may function in translocation-mediated leukemia.[10,11] Transcription factors not only regulate signaling pathways involved in a variety of physiological processes but also function in tumorigenesis in epithelial cancers.[12] Aberrant over-expression of RUNX1 has been observed in cancers, including epithelial ovarian carcinoma, glioma, and lung cancer.[13–15] However, the role of RUNX1 in HNSCC has yet to be understood.

Based on previous studies of RUNX1, we hypothesized that RUNX1 is a key player in regulating HNSCC development and progression. In this study, we evaluated RUNX1

expression in HNSCC specimens and its clinical significance. Furthermore, we examined its effects on proliferation, migration, and invasion of HNSCC.

Materials and methods

Patient

The retrospective study included 80 HNSCC patients admitted to the Affiliated Hospital of Qingdao University between 2012 and 2014. The patients were histologically examined by two independent pathologists, and the pathological stages were confirmed according to the guidance by the American Joint Committee on Cancer (AJCC). The specimens were collected with the patients' consent, and the procedures were performed under the guidance by the Independent Ethics Committee of the Affiliated Hospital of Qingdao University.

Cell lines

The SCC25 and CAL27 cells were obtained from Shanghai Ninth People's Hospital. The cells were incubated at 37 °C using the Dulbecco's Modified Eagle Media/F12 (DMEM/F12) medium with 10% fetal bovine serum (Gibco, USA).

Analysis of RUNX1 expression in published datasets

Data from the Ginos cohort were processed as described previously. The messenger ribonucleic acid (mRNA) and clinical data were acquired from the Oncomine Research Edition for Cancer Genomics (https://www.oncomine.org/).[16] The Cancer Genome Atlas (TCGA) data were acquired from the Cancer Genome Atlas Program (https://tcga-data.nci.nih.gov/tcga/), which contain the mRNA profiles from 44 normal and 497 HNHCC primary tumor samples. The mRNA profiles from the oral cavity squamous cell carcinoma with lymph node metastasis were processed by the ScanGEO program (http://scangeo.dartmouth.edu/ScanGEO/), which comprised the expression profiles of 18 oral cavity squamous cell carcinomas without or with lymph node metastasis (Gene Expression Omnibus [GEO]; GDS1062).[17] The raw data can be accessed via the GEO.

Quantitative real-time polymerase chain reaction (qPCR)

The total RNA was isolated with the TRIzol reagent (TaKaRa, Shiga, Japan). The complementary deoxyribonucleic acid was prepared, and the mRNA transcripts were analyzed by an Applied Biosystems 7900 (ABI 7900) (Foster City, CA). The relative expression was normalized to that of glyceraldehyde-3-phosphate dehydrogenase (GAPDH) with the following primers: GAPDH: sense 5′-AGAAG GCTGGGGCTCATTTG-3′, antisense 5′-AGGGGCCATCC ACAGTCTTC-3′; RUNX1: sense 5′-CTGTGATGGCTGGC AATGAT-3′, antisense 5′-TCTTCCACTTCGACCGACAA-3′.

Western blot

The proteins of the HNSCC cells were extracted using a radioimmunoprecipitation assay kit by Thermo Scientific, Rockford, IL, USA. The proteins were separated and transferred to a polyvinylidene fluoride membrane according to the Western blot protocol. The primary antibodies were β-actin (1:1000, Sigma) and RUNX1 (1:800, CST, Danvers, MA, USA).

Immunohistochemistry staining

Immunohistochemistry (IHC) staining was conducted using the primary antibodies against RUNX1 (1:200, CST) or N-cadherin (1:150, Abcam). The tissues were incubated with the Horseradish peroxidase-conjugated secondary antibody (Genetech, Shanghai, China). For RUNX1, the specimens were grouped into two groups according to the tumor cell percentages, including the low expression group ($<46\%$) and the high expression group ($\geq 46\%$). For N-cadherin, the staining intensity (SI) was scored from 0 to 3 (from weak to strong), and the staining extent (SE) was scored as 0 (0%), 1 (1–25%), 2 (26–50%), 3 (51–75%), or 4 (76–100%). The overall staining score was obtained using the SI score and SE score, based on which the specimens were classed into two groups as follows: low expression (<7) and high expression (≥ 7).

RUNX1 short hairpin ribonucleic acid interference and transfection

The short hairpin ribonucleic acid (shRNA) plasmid for RUNX1 was obtained from Genechem (Shanghai, China). The shRNA duplex sequences targeting RUNX1 (sh-RUNX1) include forward 5′-GATCCGTGCTCAACTCCC AACAAAC TTCAAGAGAGTTTGTTGGGAGTTGAGCA TTTTTTG-3′ and reverse 5′-AATTCAAAAAATGCTC AACTCCCAACAAACTCTCTTGAAGTTTGTTGGGAGT TGAGCACG-3′. The shRNA target sequence for the negative control vector (sh-Control) was 5′-GAAGCAGCA CGACTTCTTC-3′. For the selection of stable cell lines, 5×10^4 HNSCC cells were transfected with viral particles (5×10^5 transducing units/mL) for another 8 h. The stable cells expressing RUNX1 shRNA and control shRNA were selected by puromycin for seven days after transduction.

Cell counting kit-8 and colony formation assays

A total of 8 μL cell counting kit-8 (CCK-8) was added to 1×10^4 HNSCC cells cultured for 12, 24, 36, or 48 h, which were then incubated for another 2 h. The cells were counted by measuring the absorbance at 450 nm. For plate colony formation assays, 5×10^2 HNSCC cells were cultured for 12 days, and then the colonies were counted after fixed and stained with the Giemsa stain solution.

Scratch assays

The HNSCC cells achieving 80% confluence were scratched and cultured with serum-free DMEM/F12 with 10 μg/mL mitomycin-C (Sangon, Shanghai, China) for 24 h. Then, the

wound was examined using an Olympus fluorescence microscope (Japan).

Matrigel invasion assays

A total of 1×10^5 transfected cells were incubated in the upper chambers precoated with 200 µL Matrigel in the cell invasion assay, and a total of 600 µL DMEM/F12 were placed in the lower chambers. The non-invasive cells were gently removed and the other cells were stained with crystal violet dye (0.1%). The cells were counted under an inverted microscope using six randomly selected locations.

HNSCC xenograft nude mouse model

The BALB/c nude mice (Shanghai Laboratory Animal Center) were divided into two groups. In the control group, 100 µL 5×10^6 sh-Control HNSCC cells were subcutaneously injected into the flank region of the mice ($n = 8$). The mice in the other group ($n = 8$) were injected with equivalent sh-RUNX1 HNSCC cells. After five weeks, the mice were sacrificed by cervical dislocation after being anesthetized intraperitoneally with 4% chloral hydrate. The tumors were removed, and the volumes were obtained by the formula: volume (m^3) $=1/2$ length $\times$ width2. The procedures were approved by the Institutional Animal Care and Use Committee of the Affiliated Hospital of Qingdao University (approval number: 2019030602). The tumor burden did not exceed the recommended dimensions.

Statistical analyses

The pair-wise differences were determined by two-tailed Student's *t*-test SPSS 19.0 (Chicago, IL). The relationship between RUNX1 and N-cadherin expression with clinicopathological parameters was analyzed using Chi-square tests. Multivariate analysis and the

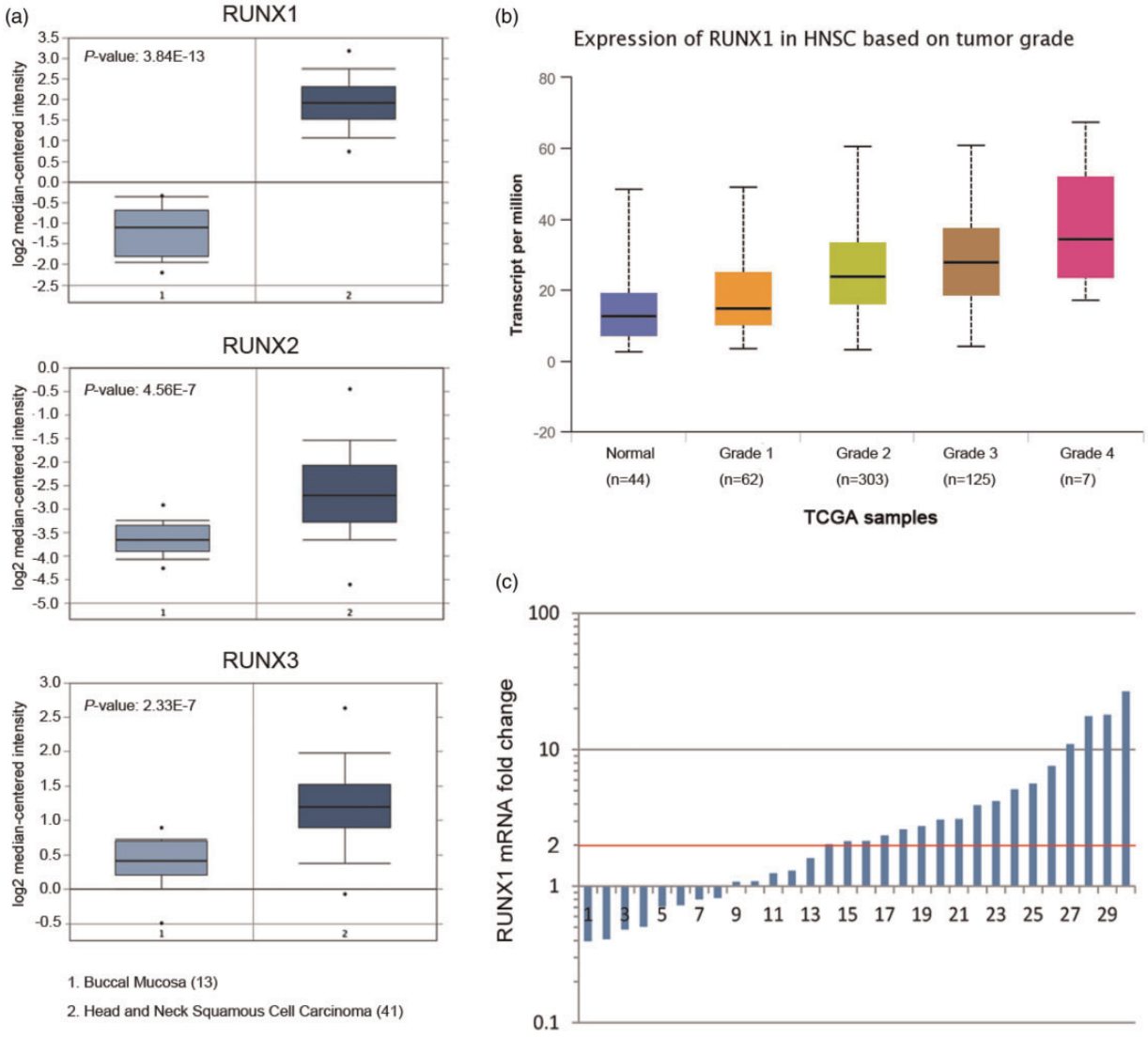

Figure 1. RUNX1 in human HNSCC specimen. (a) RUNX1, RUNX2, and RUNX3 in 13 normal buccal mucosa and 41 HNSCC. The data and *P* values were obtained from the Ginos cohort in ONCOMINE database. (b) RUNX1 in 44 normal and 497 different grades of HNSCC. The data and *P* values were obtained from the TCGA database. (c) RUNX1 in 30 HNSCC and adjacent normal tissues were determined by real-time qPCR. (A color version of this figure is available in the online journal.)

overall survival (OS) rates were performed using the Cox proportional hazards model and the Kaplan–Meier method, respectively. The survival curves were compared using the log-rank test. $P < 0.05$ was considered statistically significant.

Results

Aberrant RUNX1 over-expression in HNSCC tissues

We first searched the OncoMine database and found that RUNX1 expression was greatly elevated in HNSCC

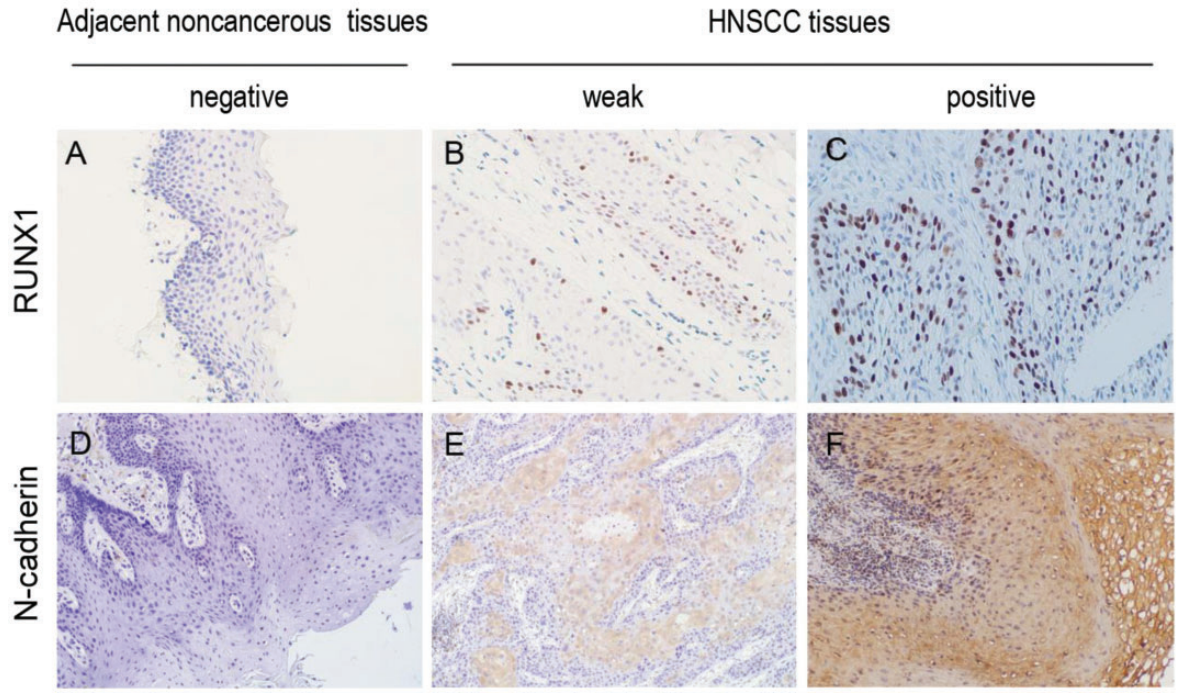

Figure 2. Immunohistochemical staining of N-cadherin and RUNX1 in HNSCC. The expression of RUNX1 (a–c) and N-cadherin (d–f) in HNSCC tissues and adjacent noncancerous tissues was examined by immunohistochemical staining (200× magnification for RUNX1 staining and 100× for N-cadherin staining). (A color version of this figure is available in the online journal.)

Table 1. Relationship clinicopathologic parameters and RUNX1 and N-cadherin expression ($n = 80$).

		RUNX1 expression			N-cadherin expression		
Parameters	**Total**	**Low (29)**	**High (51)**	**P value***	**Low (32)**	**High (48)**	**P value***
Age				0.244			0.246
<60	32	9	23		10	22	
≥60	48	20	28		22	26	
Gender				0.452			0.461
Male	55	18	37		24	31	
Female	25	11	14		8	17	
Location				0.153			0.675
Tongue	33	10	23		15	18	
Gingiva	29	9	20		10	19	
Other	18	10	8		7	11	
T stage				0.019*			0.072
T1 + T2	35	18	17		10	25	
T3 + T4	45	11	34		22	23	
N stage				0.036*			<0.001*
N0	42	20	22		25	17	
N1 + N2	38	9	29		7	31	
AJCC stage				0.021*			0.001*
I + II	44	21	23		25	19	
III + IV	36	8	28		7	29	
Differentiation				0.314			0.51
Well + moderate	70	27	43		27	43	
Poor	10	2	8		5	5	

*P values are based on Chi-square or Fisher's exact test. $P < 0.05$ indicates a significant association among the parameters.

compared with that of RUNX2 and RUNX3 (Figure 1(a)). In addition, compared with the normal tissue, RUNX1 showed high expression in HNSCC as shown in the TCGA data set, and the RUNX1 expression was increased in a tumor grade-dependent manner (Figure 1(b)). Among 30 paired HNSCC cases, 17 (56.7%, $P < 0.01$) HNSCC tissues showed a more than 2-fold increase compared with normal tissues (Figure 1 (c)), indicating that RUNX1 expression is commonly elevated in human HNSCC.

Correlation between RUNX1 expression and HNSCC clinicopathologic parameters

The expression of RUNX1 was detected in 80 primary HNSCC tissues using IHC, among which only 29 (36.3%) showed low RUNX1 expression (Figure 2(b) and (c) and Table 1). RUNX1 showed no obvious expression in adjacent tissues (Figure 2(a)). As shown in Table 1, the expression of RUNX1 is correlated with AJCC stage, N stage, and T stage.

Table 2. The association between RUNX1 and N-cadherin expression.

	N-cadherin expression			
Tissue sample	Low	High	P value	r
RUNX1 low	19	10	<0.001*	0.393
RUNX1 high	13	38		

*P values are based on Spearman's correlation coefficient test. $P < 0.05$ indicates a significant association among the parameters.

N-cadherin is critical to metastasis of tumor cells, and thus we analyzed the relationship between N-cadherin and RUNX1, which showed that the elevated expression of N-cadherin was correlated with N stage and AJCC stage of HNSCC (Figure 2(e) and (f) and Table 1). A positive correlation was observed between N-cadherin and RUNX1 ($P < 0.001$, Table 2). These observations suggest that RUNX1 and N-cadherin are correlated with HNSCC progression.

Correlation of RUNX1 expression and clinical outcomes of HNSCC

We then assessed the correlation between the OS rates of HNSCC patients and the expression of RUNX1 or N-cadherin, which showed that patients with high RUNX1 and N-cadherin expression had low OS rates ($P = 0.009$ and $P = 0.012$, respectively) compared with those with low expression of these factors (Figure 3(a) and (b)). We also found that the OS rates were low in tumors exhibiting low expression levels of both RUNX1 and N-cadherin ($P = 0.002$) (Figure 3(c)). These results demonstrated that the elevated expression of RUNX1 could be used as an independent prognostic factor for HNSCC ($P < 0.001$, Table 3).

Knockdown of RUNX1 expression suppresses HNSCC cell proliferation

Western blot analysis confirmed that the RUNX1 expression was significantly decreased in the knockdown cells

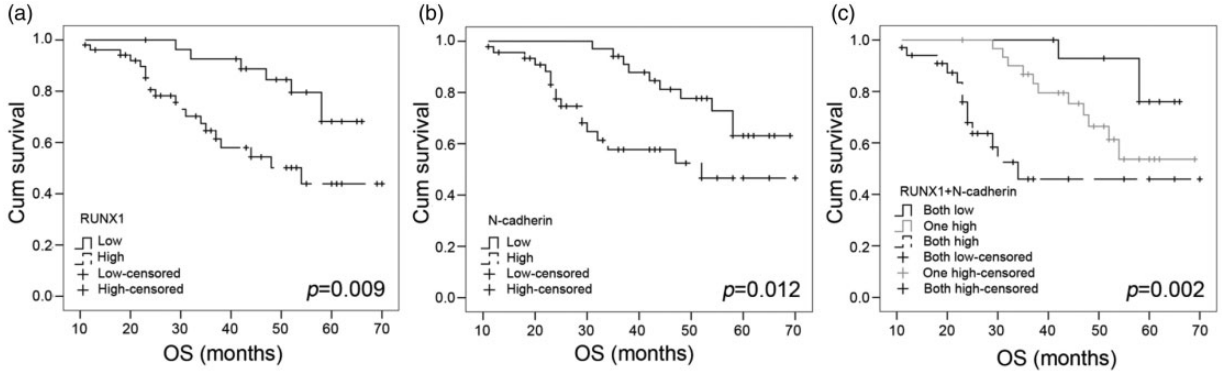

Figure 3. Kaplan–Meier analysis of HNSCC patient survival. The OS rates of patients on the basis of the immunohistochemical RUNX1 (a) and N-cadherin (b). (c) The OS rate is negatively correlated with the expression level of RUNX1 and N-cadherin.

Table 3. Multivariate Cox proportional hazard models for overall survival.

	Overall survival	
Variable	HR (95% CI)	P value
T stage (T1 + T2 vs. T3 + T4)	1.73 (1.09–4.01)	0.273
N stage (N0 vs. N1 + N2)	7.241 (2.083–18.640)	<0.001*
AJCC stage (I + II vs. III + IV)	3.879 (1.792–6.652)	0.012*
Differentiation (well vs. moderate + poor)	7.519 (3.854–14.302)	<0.001*
RUNX1 (low vs. high)	5.572 (1.860–9.963)	<0.001*
RUNX1/ N-cadherin (both low vs. both high)	8.271 (3.082–13.553)	<0.001*

HR, hazard ratio; CI, confidence interval; P values are based on Likelihood Ratio test.
*$P < 0.05$ indicates significant difference.

(Figure 4(a)). Plate colony formation assays suggested that RUNX1 knockdown significantly inhibited cell clonogenicity ($P < 0.01$, Figure 4(b)). In addition, cell growth was significantly inhibited after RUNX1 knockdown ($P < 0.05$, Figure 4(c)) as shown in the CCK-8 assay, indicating that RUNX1 could promote HNSCC cell proliferation.

RUNX1 knockdown on HNSCC cell migration and invasion

Since RUNX1 is linked to lymph node metastasis in HNSCC, the function of RUNX1 on cell migration and invasion was further investigated by scratch assays using SCC25 and CAL27 cells (Figure 5(a)). Matrigel invasion assays demonstrated that knockdown of RUNX1 resulted in a significantly lower invasive ability ($P < 0.01$, Figure 5 (b)). In the O'Donnel clinical cohort, expression of RUNX1 was increased in lymph node metastasis and HNSCC metastasis samples compared with non-metastatic samples ($P = 0.001$, Figure 5(c)). These results support that HNSCC cell migration and invasion may be potently dampened by RUNX1 knockdown.

RUNX1 knockdown represses HNSCC progression in vivo

The effect of RUNX1 on HNSCC progression was evaluated by RUNX1 knockdown using sh-RUNX1 and sh-Control. The experimental scheme is shown in Figure 6(a). As shown in Figure 6(b)–(d), the sh-RUNX1 tumors were markedly smaller both in size and weight than the sh-Control tumors. Furthermore, N-cadherin and vimentin showed a decreased expression in the sh-RUNX1-transfected HNSCC xenografts (Figure 6(e)). These results showed that RUNX1 knockdown could repress HNSCC metastasis *in vivo*.

Discussion

As a common cancer,[18] HNSCC can be developed from multiple alterations of gene expression, though the molecular mechanism is yet to be fully understood.[19] Our study uncovers that RUNX1 functioned in proliferation and invasion of HNSCC, and high expression of RUNX1 was correlated with lymph node metastasis, AJCC stage, and tumor size, implicating RUNX1 can be used as a biomarker of malignant tumors. Furthermore, our results indicate that RUNX1 knockdown markedly repressed HNSCC cell proliferation, migration, and invasion. However, the downstream mechanisms need to be further investigated.

It is well accepted that invasion and metastasis are important factors in tumor progression, and this progression depends on the invasion ability of tumor cells.[20] It has been shown that activation of invasion can be one of the initialization steps of cancer,[21] which is driven by inactivation of tumor suppressors and activation of oncogenes as well as transcription factors aberrations.[22] Transcription factors function as either transcriptional repressors or activators by binding to DNA at specific sites,[23] which are essential in embryogenesis, tumorigenesis, invasion, and metastasis.[24,25] Among the three human RUNX genes,[3] RUNX1 has been well characterized. Although dysfunction of RUNX1 has been previously observed in hematological disorders, recent studies indicate that RUNX1 may function in migration and invasion in various solid tumors.[26,27] Keita *et al.* showed that RUNX1 expression is significantly increased not only in metastatic tissues derived from epithelial ovarian cancer (EOC) patients but also in tumors with low malignant potential. Furthermore, suppression of RUNX1 inhibited EOC cell migration and invasion.[13] Another study has shown that over-expression of RUNX1 leads to the formation of neurofibromatosis type 1 in human neurofibroma initiation cells.[28] Wang *et al.* have shown that RUNX1 impairs the inhibitory effects of miR-

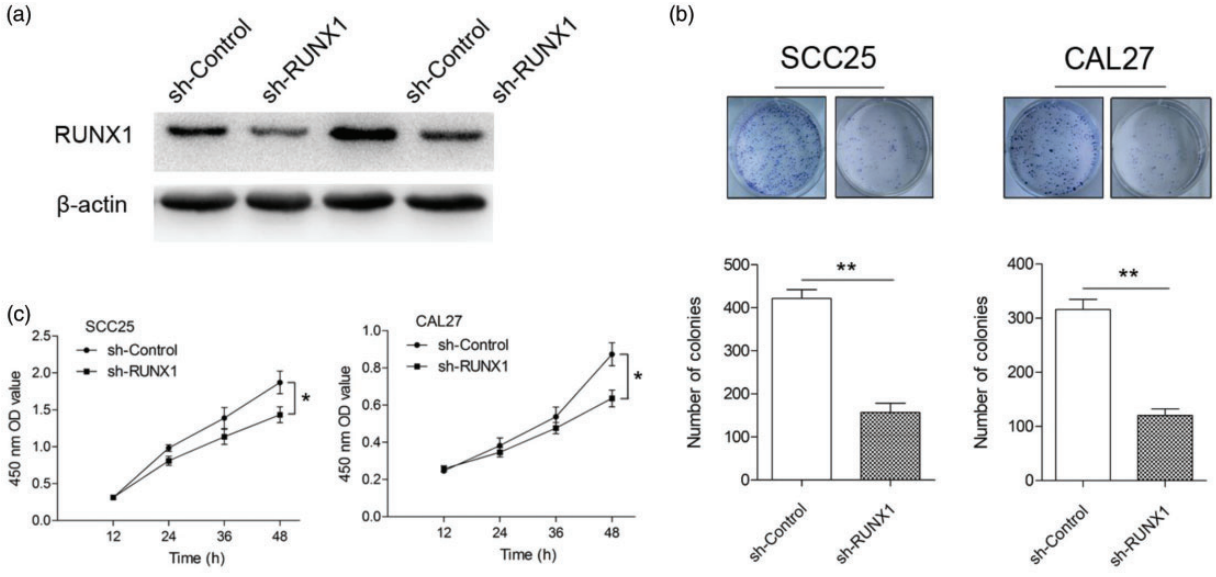

Figure 4. RUNX1 on HNSCC cell proliferation. (a) sh-RUNX1 or control shRNA-treated SCC25 and CAL27 cells. The transfection efficiency was assessed by Western blot, and the influence of RUNX1 knockdown was evaluated with plate colony formation assays (b) and CCK-8 assays (c). *$P < 0.05$ and **$P < 0.01$. (A color version of this figure is available in the online journal.)

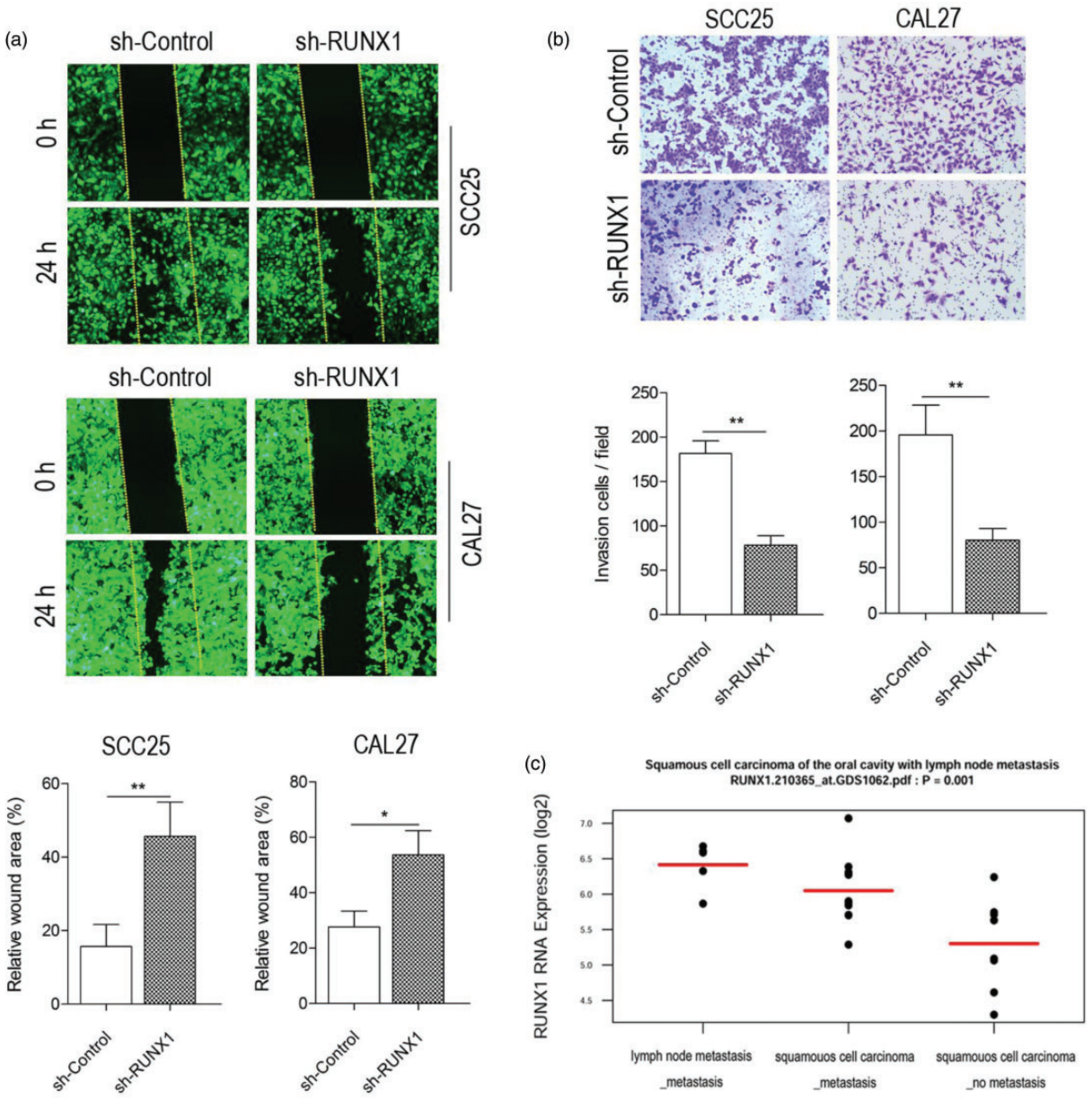

Figure 5. HNSCC cell migration and invasion by RUNX1. Scratch assays (a) and Matrigel invasion assay (b) of HNSCC cells treated with sh-RUNX1. (c) Expression levels of RUNX1 in lymph node metastasis tissues and squamous cell carcinoma of the oral cavity with or without lymph node metastasis in the O'Donnel clinical cohort. The mean is indicated with a red line. $^{*}P < 0.05$ and $^{**}P < 0.01$. (A color version of this figure is available in the online journal.)

101 on lung cancer invasion.[29] We confirmed that RUNX1 had elevated expression in primary HNSCC tissues, which was associated with the N stage and AJCC stage. In addition, our results show that RUNX1 knockdown could inhibit HNSCC migration and invasion.

Sustaining proliferative signaling is another critical hallmark of cancer.[21] The effect of RUNX1 in tumor proliferation has also drawn wide attention from researchers. Scheitz *et al.* found that Runx1 activates the Stat3 signaling pathway by directly inhibiting the transcription of cytokine signaling 3 (SOCS3) and SOCS4, which is an essential step for the proliferation of cancer cell. Studies have shown that RUNX1 knockdown inhibits the initiation of epithelial cancer cells of oral, skin, and ovarian.[30] On the other hand, RUNX1 activation promotes colorectal cancer cell proliferation.[31] In this study, we showed that the size of primary tumors (T stage) was significantly correlated with the RUNX1 expression level ($P = 0.019$). RUNX1 knockdown suppressed the proliferation activity of SCC25 and CAL27 cells and reduced colony formation ability. According to the *in vitro* results above, we then investigated the tumorigenicity of sh-RUNX1 and sh-Control cells in nude mice, which indicated that the downregulation of RUNX1 inhibited the formation of subcutaneous tumors *in vivo*. These data indicate that suppression of RUNX1 could inhibit HNSCC cell proliferation. However, the diagnostics relies on tissue biopsy and the histopathology has some inadequacies. For example, the specimen

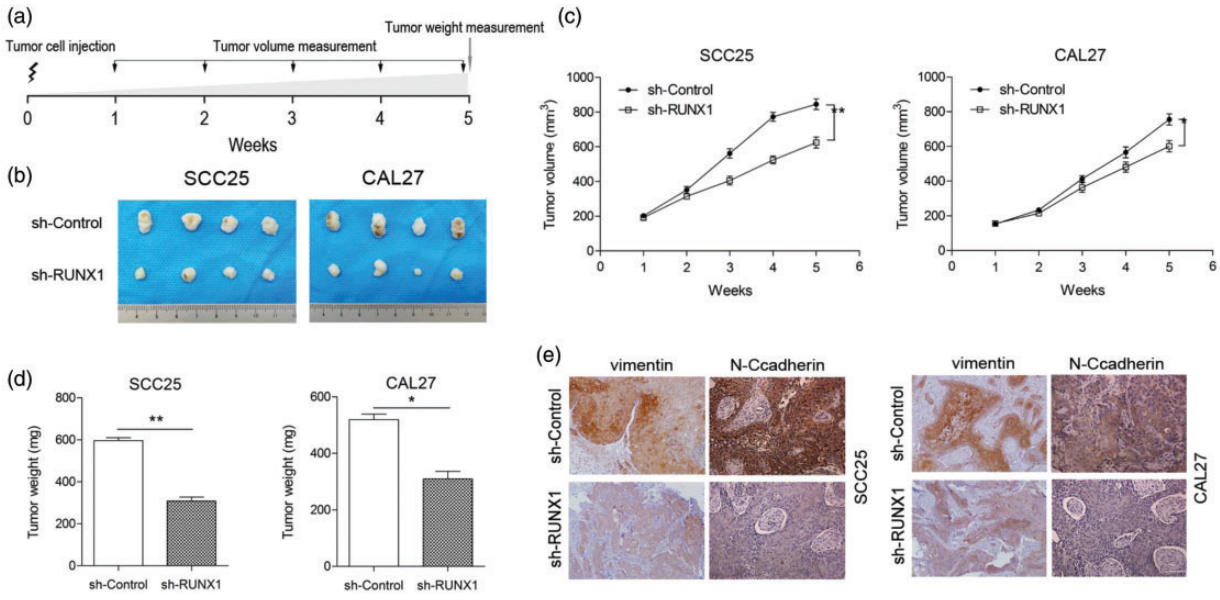

Figure 6. RUNX1 on HNSCC xenograft growth and metastasis. (a) Schematic representation for the establishment of HNSCC cell injection and tumor volume and weight measurement. (b) Representative images of HNSCC cell tumors expressing sh-RUNX1 or sh-Control. (c) The growth curves of xenograft tumors expressing sh-RUNX1 or Control shRNA. (d) The weight changes of the subcutaneous tumors harvested at week 5. (e) N-cadherin and vimentin in sh-RUNX1 or sh-Control-treated tumors. $^{*}P < 0.05$ and $^{**}P < 0.01$. (A color version of this figure is available in the online journal.)

acquisition is invasive and painful, and the progression of the disease significantly delays the treatment. New diagnostic methods should be developed for this purpose, such as saliva, which, as an inexhaustible biofluid, includes unprecedentedly rich genetic information.[32] Our results demonstrated that RUNX1 mRNA in HNSCC was increased compared with that in the normal tissues. Further experiments will be conducted to determine whether the mRNA of RUNX1 in saliva could be used as a biomarker for the diagnosis of HNSCC.

The limitations of the experimental design are discussed. First, the total RNA of different samples was compared using GAPDH as the control. However, the expression of GAPDH may show different variability in different cells.[33] Therefore, a second housekeeping gene (such as β-actin [ACTB]) needs to be used as an internal reference. Second, according to the prospective-specimen collection, retrospective-blinded-evaluation design for biomarker studies by Pepe *et al*., the results in this study need to be further validated with a large, prospective, controlled clinical study.[34]

In conclusion, our study has identified that RUNX1 is a new tumor-promoting transcription factor, which plays a significant role in the proliferation and metastasis of HNSCC cells. Thus, RUNX1 may be used as a sensitive biomarker for tumor recurrence and prognosis in patients with HNSCC.

AUTHORS' CONTRIBUTIONS

X.F. and Z.Z. performed data acquisition and manuscript preparation. Z.Z. collected and embedded the clinical specimens. Y.W. and G.S. participated in the animal experiments. L. W. polished the manuscript. J.Z. and Q.W. helped in statistical analysis. L.L. revised the manuscript.

DECLARATION OF CONFLICTING INTERESTS

The author(s) declared no potential conflicts of interest with respect to the research, authorship, and/or publication of this article.

ETHICAL APPROVAL

The study was carried out in accordance with the Declaration of Helsinki. All HNSCC patients in this study provided the informed consent. The experimental protocols were approved by the Ethics Committee of The Affiliated Hospital of Qingdao University (Qingdao, China).

FUNDING

The author(s) disclosed receipt of the following financial support for the research, authorship, and/or publication of this article: This study was supported by the National Natural Science Foundation of China (no. 82002226), the China Postdoctoral Science Foundation (no. 2019M652330) and the Affiliated Hospital of Qingdao University Outstanding Young Scientists Foundation (no. 3054).

ORCID iD

Xiaodong Feng https://orcid.org/0000-0003-2700-8304

REFERENCES

1. Siegel RL, Miller KD, Jemal A. Cancer statistics, 2020. *CA Cancer J Clin* 2020;**70**:7–30
2. Sato H, Tsukahara K, Okamoto I, Katsube Y, Shimizu A, Kondo T, Hanyu K, Fushimi C, Okada T, Miura K. Clinical outcomes of platinum-based chemotherapy plus cetuximab for recurrent or metastatic squamous cell carcinoma of the head and neck: comparison between platinum-sensitive and platinum-resistant patients. *Acta Otolaryngol* 2019;**22**:1–5

3. Chuang LS, Ito K, Ito Y. RUNX family: regulation and diversification of roles through interacting proteins. *Int J Cancer* 2013;**132**:1260–71
4. Deltcheva E, Nimmo R. RUNX transcription factors at the interface of stem cells and cancer. *Biochem J* 2017;**474**:1755–68
5. Ichikawa M, Yoshimi A, Nakagawa M, Nishimoto N, Watanabe-Okochi N, Kurokawa M. A role for RUNX1 in hematopoiesis and myeloid leukemia. *Int J Hematol* 2013;**97**:726–34
6. Maki K, Sasaki K, Sugita F, Nakamura Y, Mitani K. Acute myeloid leukemia with t(7;21)(q11.2;q22) expresses a novel, reversed-sequence RUNX1-DTX2 chimera. *Int J Hematol* 2012;**96**:268–73
7. Booth CAG, Barkas N, Neo WH, Boukarabila H, Soilleux EJ, Giotopoulos G, Farnoud N, Giustacchini A, Ashley N, Carrelha J, Jamieson L, Atkinson D, Bouriez-Jones T, Prinjha RK, Milne TA, Teachey DT, Papaemmanuil E, Huntly BJP, Jacobsen SEW, Mead AJ. Ezh2 and Runx1 mutations collaborate to initiate Lympho-Myeloid leukemia in early thymic progenitors. *Cancer Cell* 2018;**33**:274–91
8. Huang X, Peng JW, Speck NA, Bushweller JH. Solution structure of core binding factor beta and map of the CBF alpha binding site. *Nat Struct Biol* 1999;**6**:624–7
9. Wong WF, Kohu K, Chiba T, Sato T, Satake M. Interplay of transcription factors in T-cell differentiation and function: the role of Runx. *Immunology* 2011;**132**:157–64
10. Wang L, Sun Y, Meng L, Xu X. First case of AML with rare chromosome translocations: a case report of twins. *BMC Cancer* 2018;**18**:458
11. Yamato G, Shiba N, Yoshida K, Hara Y, Shiraishi Y, Ohki K, Okubo J, Park MJ, Sotomatsu M, Arakawa H, Kiyokawa N, Tomizawa D, Adachi S, Taga T, Horibe K, Miyano S, Ogawa S, Hayashi Y. RUNX1 mutations in pediatric acute myeloid leukemia are associated with distinct genetic features and an inferior prognosis. *Blood* 2018;**131**:2266–70
12. Chen KS, Lim JWC, Richards LJ, Bunt J. The convergent roles of the nuclear factor I transcription factors in development and cancer. *Cancer Lett* 2017;**410**:124–38
13. Keita M, Bachvarova M, Morin C, Plante M, Gregoire J, Renaud MC, Sebastianelli A, Trinh XB, Bachvarov D. The RUNX1 transcription factor is expressed in serous epithelial ovarian carcinoma and contributes to cell proliferation, migration and invasion. *Cell Cycle* 2013;**12**:972–86
14. Teng H, Wang P, Xue Y, Liu X, Ma J, Cai H, Xi Z, Li Z, Liu Y. Role of HCP5-miR-139-RUNX1 feedback loop in regulating malignant behavior of glioma cells. *Mol Ther* 2016;**24**:1806–22
15. Chen Y, Zhang L, Liu L, Sun S, Zhao X, Wang Y, Zhang Y, Du J, Gu L. Rasip1 is a RUNX1 target gene and promotes migration of NSCLC cells. *Cancer Manag Res* 2018;**10**:4537–52
16. Ginos MA, Page GP, Michalowicz BS, Patel KJ, Volker SE, Pambuccian SE, Ondrey FG, Adams GL, Gaffney PM. Identification of a gene expression signature associated with recurrent disease in squamous cell carcinoma of the head and neck. *Cancer Res* 2004;**64**:55–63
17. Koeppen K, Stanton BA, Hampton TH. ScanGEO: parallel mining of high-throughput gene expression data. *Bioinformatics* 2017;**33**:3500–1
18. Siegel RL, Miller KD, Jemal A. Cancer statistics, 2017. *CA Cancer J Clin* 2017;**67**:7–30
19. Qiu YL, Liu YH, Ban JD, Wang WJ, Han M, Kong P, Li BH. Pathway analysis of a genomewide association study on a long noncoding RNA expression profile in oral squamous cell carcinoma. *Oncol Rep* 2019;**41**:895–907
20. Polyak K, Weinberg RA. Transitions between epithelial and mesenchymal states: acquisition of malignant and stem cell traits. *Nat Rev Cancer* 2009;**9**:265–73
21. Hanahan D, Weinberg RA. Hallmarks of cancer: the next generation. *Cell* 2011;**144**:646–74
22. Schmalhofer O, Brabletz S, Brabletz T. E-cadherin, beta-catenin, and ZEB1 in malignant progression of cancer. *Cancer Metastasis Rev* 2009;**28**:151–66
23. Latchman DS. Transcription factors: an overview. *Int J Biochem Cell Biol* 1997;**29**:1305–12
24. Taube JH, Herschkowitz JI, Komurov K, Zhou AY, Gupta S, Yang J, Hartwell K, Onder TT, Gupta PB, Evans KW, Hollier BG, Ram PT, Lander ES, Rosen JM, Weinberg RA, Mani SA. Core epithelial-to-mesenchymal transition interactome gene-expression signature is associated with claudin-low and metaplastic breast cancer subtypes. *Proc Natl Acad Sci U S A* 2010;**107**:15449–54
25. Ito Y, Bae SC, Chuang LS. The RUNX family: developmental regulators in cancer. *Nat Rev Cancer* 2015;**15**:81–95
26. Micol JB, Duployez N, Boissel N, Petit A, Geffroy S, Nibourel O, Lacombe C, Lapillonne H, Etancelin P, Figeac M, Renneville A, Castaigne S, Leverger G, Ifrah N, Dombret H, Preudhomme C, Abdel-Wahab O, Jourdan E. Frequent ASXL2 mutations in acute myeloid leukemia patients with t(8;21)/RUNX1-RUNX1T1 chromosomal translocations. *Blood* 2014;**124**:1445–9
27. Otalora-Otalora BA, Henriquez B, Lopez-Kleine L, Rojas A. RUNX family: oncogenes or tumor suppressors (Review). *Oncol Rep* 2019;**42**:3–19
28. Li H, Zhao X, Yan X, Jessen WJ, Kim MO, Dombi E, Liu PP, Huang G, Wu J. Runx1 contributes to neurofibromatosis type 1 neurofibroma formation. *Oncogene* 2016;**35**:1468–74
29. Wang X, Zhao Y, Qian H, Huang J, Cui F, Mao Z. The miR-101/RUNX1 feedback regulatory loop modulates chemo-sensitivity and invasion in human lung cancer. *Int J Clin Exp Med* 2015;**8**:15030–42
30. Scheitz CJ, Lee TS, McDermitt DJ, Tumbar T. Defining a tissue stem cell-driven Runx1/Stat3 signalling axis in epithelial cancer. *EMBO J* 2012;**31**:4124–39
31. Zhou Y, Zhang X, Zhang J, Fang J, Ge Z, Li X. LRG1 promotes proliferation and inhibits apoptosis in colorectal cancer cells via RUNX1 activation. *PLoS One* 2017;**12**:e0175122 [10.1371/journal.pone.0175122]
32. Aro K, Kaczor-Urbanowicz K, Carreras-Presas CM. Salivaomics in oral cancer. *Curr Opin Otolaryngol Head Neck Surg* 2019;**27**:91–7
33. Kaczor-Urbanowicz KE, Trivedi HM, Lima PO, Camargo PM, Giannobile WV, Grogan TR, Gleber-Netto FO, Whiteman Y, Li F, Lee HJ, Dharia K, Aro K, Martin Carreras-Presas C, Amuthan S, Vartak M, Akin D, Al-Adbullah H, Bembey K, Klokkevold PR, Elashoff D, Barnes VM, Richter R, DeVizio W, Masters JG, Wong DTW. Salivary exRNA biomarkers to detect gingivitis and monitor disease regression. *J Clin Periodontol* 2018;**45**:806–17
34. Pepe MS, Feng Z, Janes H, Bossuyt PM, Potter JD. Pivotal evaluation of the accuracy of a biomarker used for classification or prediction: standards for study design. *J Natl Cancer Inst* 2008;**100**:1432–8

(Received June 4, 2020, Accepted September 26, 2020)